The Value of Quantitative Analysis of Glucose Utilization in Detection of Myocardial Viability by PET

M. Juhani Knuuti, Pirjo Nuutila, Ulla Ruotsalainen, Mika Teräs, Markku Saraste, Risto Härkönen, Aapo Ahonen, Uno Wegelius, Arto Haapanen, Jörgen Bergman, Merja Haaparanta and Liisa-Maria Voipio-Pulkki

Turku Medical Cyclotron-PET Center and Departments of Nuclear Medicine, Clinical Physiology, Radiology and Medicine, Turku University Central Hospital, Turku, Finland

To study whether absolute quantitation of regional myocardial glucose utilization (rMGU) enhances detection of myocardial viability, 70 nondiabetic patients with prior myocardial infarction and angiographically confirmed coronary artery disease were studied with [^{18}F]FDG PET after oral glucose loading. Forty-eight patients were also revascularized and underwent echocardiography after revascularization to detect wall motion recovery. The rMGU was calculated in eight myocardial segments in each patient and the results were compared to normalized (relative) [^{18}F]FDG uptake values. In normal segments (n = 225), rMGU was 56 ± 18 μmole/min/100 g (mean ± s.d.) and relative [^{18}F]FDG uptake 97% ± 12%. The interindividual variation of rMGU in normal myocardium was greater than the intraindividual variation (s.d. 31% versus 11%). The respective values for relative [^{18}F]FDG uptake were 9% and 10%. Both rMGU and [^{18}F]FDG uptake were significantly reduced in segments with scarring observed visually during bypass surgery (29 ± 19 μmole/min/100 g and 45% ± 22%, n = 26). The rMGU and [^{18}F]FDG uptake were higher in segments that recovered after revascularization (53 ± 17 μmole/min/100/g and 110% ± 21%, n = 27) than in those that did not (37 ± 20 μmole/min/100 g and 65% ± 24%, n = 63). However, due to larger variability of rMGU values, normalized [^{18}F]FDG uptake was superior to rMGU in separating normal and scar segments as well as in predicting wall motion recovery. We conclude that rMGU variability is notable and is caused mainly by variations between patients. Interindividual variation is reduced by normalization, which results in more accurate assessment of myocardial viability. Thus, static imaging and semiquantitative analysis are sufficient for the clinical assessment of myocardial viability.

J Nucl Med 1993; 34:2068-2075

$\mathbf{P}$ET imaging of the heart with [^{18}F]-2-fluoro-2-deoxy-D-glucose ([^{18}F]FDG) has been widely used to assess myocardial viability in patients with myocardial infarction (1-19).

Variable methods for analyzing myocardial images have been used. The analysis is often qualitative, with visual comparison of segmental [^{18}F]FDG uptake to that of a perfusion tracer (6-9,13) or the segmental ratio of [^{18}F]FDG uptake and flow that has been calculated (1-5,7-10,13,17-19). A semiquantitative approach by normalizing [^{18}F]FDG uptake to the segment with maximum flow has also been used (12,14-17). The recent development of a method to derive regional myocardial glucose utilization rates (rMGU) from [^{18}F]FDG PET data (20-23) has made it possible to measure rMGU noninvasively in humans. This method has been suggested in many studies and reportedly allows more accurate determination of the amount of viable tissue (1,3,5,9-11,13,15,18,19). Although this method requires dynamic PET imaging and is more complicated than measuring static [^{18}F]FDG uptake, it has potential advantages. In addition to being a physiological variable, rMGU accounts for the [^{18}F]FDG dose, imaging time, patient size and plasma glucose levels without requiring information about myocardial perfusion. However, the accuracy of this approach in detecting myocardial viability has not been studied.

The purpose of this study was: (1) to assess the value of absolute quantitation of rMGU in studies of myocardial viability and (2) to compare those results to semiquantitative analysis of [^{18}F]FDG uptake, which is widely used in viability studies (12,14-17).

METHODS

Subjects

The study group consisted of 70 consecutive nondiabetic patients with stable angiographically confirmed coronary artery disease. All patients had a prior myocardial infarction (Table 1). All patients had a wall motion abnormality at rest detected by echocardiography or cineventriculography. The mean interval between the myocardial infarction and the PET study was 14 mo (range 3-120 mo).

Study Protocol

All 70 patients underwent PET imaging with [^{18}F]FDG. Sixty-four patients also underwent SPECT perfusion imaging at rest.

TABLE 1
Patient Characteristics

Sex (male/female)	67/3
Age (yr, mean ± s.d.)	53 ± 9
Myocardial infarction	70 (100%)
ECG Q-wave MI	45 (64%)
Anterior wall MI	35 (50%)
Inferior or posterior wall MI	35 (50%)
NYHA class	2.2 ± 0.8
EF	51 ± 11%
Coronary anatomy	
One-vessel disease	15 (21%)
Two-vessel disease	12 (17%)
Three-vessel disease	43 (61%)
Medications	
Nitrates	58 (83%)
Beta-blockers	57 (81%)
Calcium antagonists	38 (54%)
Revascularization	48 (87%)
Coronary bypass	37 (67%)
Angioplasty	11 (20%)

ECG = electrocardiography; EF = left ventricular ejection fraction in cineangiography (available in 55 patients); MI = myocardial infarction.

Echocardiography was performed on the same day as PET imaging in 53 patients and it was repeated 2–6 mo after coronary bypass surgery (3–8 wk after angioplasty) in the 48 patients who were subsequently revascularized. The decision to perform revascularization had been made without knowledge of the PET and echocardiographic results. Coronary angiography was performed 1.6 ± 1.3 mo prior to the PET study (all within 4 mo). The time interval between the PET and SPECT studies was 2.2 ± 3.7 mo and 2.2 ± 1.9 mo between the PET study and revascularization (in 96% of patients within 4 mo). None of the patients experienced unstable angina or myocardial infarction between the studies, the revascularization procedure and follow-up echocardiography. Each subject gave written informed consent and the study protocol was accepted by the Ethical Committee of the Turku University Central Hospital.

PET Study

All studies were performed after a 12-hr overnight fast. Patients took only nitrates, if needed, for at least 24 hr prior to the PET study. The patients ingested 50 g of glucose 60 min before tracer injection. Two catheters were inserted, one in an antecubital vein for injection of [18F]FDG and the other in a contralateral hand vein of the upper extremity that was warmed (70°C) for sampling of arterialized venous blood. Plasma glucose was determined every 10 min from arterialized venous blood.

Preparation of [18F]FDG. Fluorine-18-FDG was synthesized with an automatic apparatus by a modified method of Hamacher et al. (24). The 18F-F− had a specific activity of 5500 GBq/μmole (150 Ci/μmole) (25,26); radiochemical purity exceeded 99%.

Image Acquisition. The patients were positioned supine with their arms within the field of view in an eight-ring ECAT 931/08 tomograph (Siemens/CTI Corp., Knoxville, TN) with a measured axial resolution of 6.7 mm and 6.5 mm inplane. To correct for photon attenuation, transmission scanning was performed for 25–30 min prior to emission imaging with a removable ring source containing 68Ge (total counts 15–30 × 10^6 per plane). Sixty minutes after oral glucose loading, 240 ± 50 MBq (6.6 ± 1.6 mCi) of

[18F]FDG was injected intravenously over 15–30 sec and dynamic imaging followed for 60 min (8 × 15 sec, 2 × 30 sec, 2 × 120 sec, 1 × 180 sec, 4 × 300 sec, 3 × 600 sec). Twenty-five blood samples were taken for measurement of radioactivity in plasma.

Image Processing and Corrections. All data were corrected for deadtime, decay and photon attenuation and reconstructed in a 256 × 256 matrix. The final inplane resolution in reconstructed and Hann-filtered images was 8 mm FWHM. Thirty-five to 40 elliptical regions of interest (ROIs) were placed on representative transaxial ventricular slices in each patient (typically 4–6 ROIs of 2–4 cc per plane), avoiding myocardial borders; the time-activity curves were calculated. Myocardial time-activity curves were corrected for partial volume effects using information from echocardiographical measurements of wall thickness and left ventricular diameter and phantom studies (27,28). Plasma time-activity curves were generated from the calibrated arterialized venous blood samples by a nonlinear least squares fitting routine; this information yielded the tracer input curve.

Calculation of Regional GU. Plasma and tissue time-activity curves were analyzed graphically (22). The slope of the plot in the graphical analysis is equal to the utilization constant of [18F]FDG, K_i, which represents the fractional rate of tracer transport and phosphorylation. In this study, the last six time points representing the time 15–60 min after injection were used to determine the slope by linear regression. The myocardium was divided into eight segments as previously described (29) (anterobasal, anterior, anteroseptal, lateral, inferoseptal, apical, inferior and posterobasal). The mean K_i for each segment was derived from three to five ROIs. The rate of myocardial glucose uptake in each segment was given by $K_i * P_{gluc}/LC$, where P_{gluc} is mean plasma glucose level during imaging and LC (lumped constant) was used to correct for differences in the transport and metabolism of [18F]FDG and glucose (30–32). In this study, LC was assumed to be 0.67 (30).

Calculation of Normalized (Relative) [18F]FDG Uptake. The partial-volume corrected mean count value during 30–60 min after tracer injection in each segment was used for further calculations. Assuming that glucose uptake is normal in myocardial regions with noncompromized blood flow, [18F]FDG uptake was normalized relative to the segment uptake with the highest tracer uptake observed visually in resting SPECT perfusion imaging (typically an anterior or lateral segment). In those six patients with no SPECT imaging, the noninfarcted lateral or anterior segment supplied by a normal or nonsignificantly stenosed coronary artery was used as a reference. To study the effect of normalization, we also calculated the respective relative rMGU values.

Coronary Angiography

All patients underwent selective coronary angiography by standard techniques. A 50% or greater visual diameter reduction in a major epicardial branch was considered significant. Simultaneous two-view ventriculography was also performed in 55 patients to assess global left ventricular function. Angiography was not repeated after revascularization.

Echocardiography

Echocardiography (Aloka SSD 870, Aloka Inc, Japan or Acuson 128XP/5, Acuson Inc., CA) was performed according to the semiquantitative method recommended by the American Society of Echocardiography Committee on Standards (33) with a modified segmental subdivision (29). All standardized long-axis and short-axis echocardiographic views were obtained and videotaped. Echocardiographic analysis reproducibility was also confirmed by reanalysis of videotape recordings in 12 patients.

Quantitation of Glucose Uptake for Myocardial Viability • Knuuti et al.

2069

Echocardiograms were analyzed visually by a blinded, experienced physician. The results of individual pre- and postintervention echocardiographies were verified by comparison of paired videotape recordings. Segmental left ventricular wall motion and systolic thickening was visually scored according to the following scale: (1) normal, (2) hypokinetic wall motion with systolic thickening, (3) akinetic wall motion with no systolic thickening and (4) dyskinetic motion with no systolic thickening. The segment was classified into a higher class of abnormality if one-third of the segment showed respective findings. After revascularization, improvement of contractile function was diagnosed if systolic thickening (corresponding to score 1 or 2) became apparent in a segment that had been akinetic or dyskinetic or if normal motion was detected in a previously hypokinetic segment. Improvement in function was acknowledged only if it was apparent in a central area of the segment. Special emphasis was focused on the anteroseptal segments because postsurgical wall motion abnormalities are common in this area (34). Thus, the appearance of postoperative anteroseptal hypokinesia was regarded as normal, and improvement was recognized only if systolic thickening became apparent in a previously akinetic or dyskinetic segment or if hypokinesia was normalized.

SPECT Perfusion Imaging

Sixty-four patients underwent myocardial SPECT perfusion imaging at rest. Thallium-201 was used in 33 patients and ^{99m}Tc-MIBI was used in 31 patients. One millicurie of ^{201}Tl or 20 mCi of ^{99m}Tc MIBI was injected 1 hr before imaging in all but two patients who were studied at rest 4 hr after ^{201}Tl stress imaging (4-hr washout). SPECT images were obtained on a Siemens-Rota SPECT gamma camera (Siemens Gammasonics, Hoffman Estates, IL). The radioactivity in the eight anatomic segments was assessed qualitatively and blindly by two experienced nuclear medicine specialists. The results from resting images were scored according to the following scale: (1) normal, (2) mild defect, (3) moderate defect and (4) severe or complete defect. Discordances were resolved by simultaneous reanalysis.

Visual Inspection of Myocardium During Bypass Operation

Myocardial scars were visually detected and localized during bypass surgery without knowledge of the results of the other studies. A pale and firm area was considered to be scarred. A segment was regarded as revascularized if a corresponding major epicardial coronary artery branch had undergone a successful procedure.

Alignment of Results Obtained by Different Methods

The SPECT and PET transaxial slices were visually aligned and compared to each other. The results of the transaxial images were assigned to the eight segments with a heart map phantom. Wall motion abnormalities on echocardiograms and the visually detected scars were also localized in the segmental heart map phantom. All results were first localized by the physician responsible for each study. Segmental results from each method were finally aligned and pooled together by the first author.

Classification of Myocardial Segments

For the purpose of this study, echocardiography and SPECT first results were used to find normal myocardial segments as precisely as possible. To avoid errors induced by misalignment, only segments with concordant results by all modalities were classified as normal in this study. Thus, normal segments in this study were selected by first choosing the segments with less than 75% stenosis in the corresponding major epicardial coronary artery and then excluding from these the segments with any abnormal finding on the SPECT perfusion study or echocardiography. The scarring observed during bypass surgery was used as an indicator of severely injured myocardium and the normal segments were compared to these scarred segments.

Echocardiographic results were then used to detect functional recovery. The segments with initially abnormal wall motion in echocardiography were divided into reversible or irreversible based on the results in follow-up echocardiography.

Analytical Procedures

Plasma glucose was determined in duplicate by the glucose oxidase method (35) using a Beckman Glucose Analyzer II (Beckman Instruments, Fullerton, CA) or an Analox GM7 (Analox Instruments Ltd., Denmark).

Statistical Analysis

Independent variables were compared by analysis of variance and Bonferroni testing. All results were expressed as mean values and standard deviations. To test and compare different parameters in separating segment groups, the discriminant analysis of the SAS statistical program was used (SAS Institute Inc., Cary, NC). Sensitivities and specificities of functional recovery for different [^{18}F]FDG uptake and rMGU limit values were calculated in the segments with initially abnormal wall motion that underwent revascularization. Pearson correlation coefficients were used.

RESULTS

Fluorine-18-FDG Uptake and rMGU in Normal Segments

By definition, 560 myocardial segments in 70 patients were studied. The number of normal segments by all non-PET methods was 225 (40%). At least one segment in each patient was classified as normal, the mean number being 3.2 ± 1.6. In these segments rMGU was 56 ± 18 μmole/min/100 g (Fig. 1A) and the relative uptake of [^{18}F]FDG was 97% ± 12% (Fig. 1B). The variability of rMGU expressed as %s.d. of mean was higher than that of relative [^{18}F]FDG uptake (s.d. 31% versus 13%). This difference was not due to the segmental variation of the results, since the mean values and standard deviations of these two parameters were concordant in different segment types (Fig. 2). By both methods, the mean uptake was lowest in apical segments (p < 0.05).

The intraindividual variation was estimated as the s.d. of normal segments in patients with ≥2 such segments (n = 46). The intraindividual s.d. of rMGU was 6.3 μmole/min/100 g (11.4%) and the s.d. of relative [^{18}F]FDG uptake was 9.4% (9.7% of the mean uptake value). The interindividual variation was estimated as the s.d. of average normal values in each patient. The interindividual s.d. of rMGU was 17.3 μmole/min/100 g (31.2%) in patients with at least two normal segments (n = 46) and 18.6 μmole/min/100 g (34.0%) in all patients (n = 70). These values were higher than the respective results for relative [^{18}F]FDG uptake (8.6% and 8.7%). To study whether the observed difference in the interindividual variabilities was dependent on the normalization procedure, normalized rMGU values were calculated using the same reference segments used to normalize [^{18}F]FDG uptake values. Variabilities obtained by both
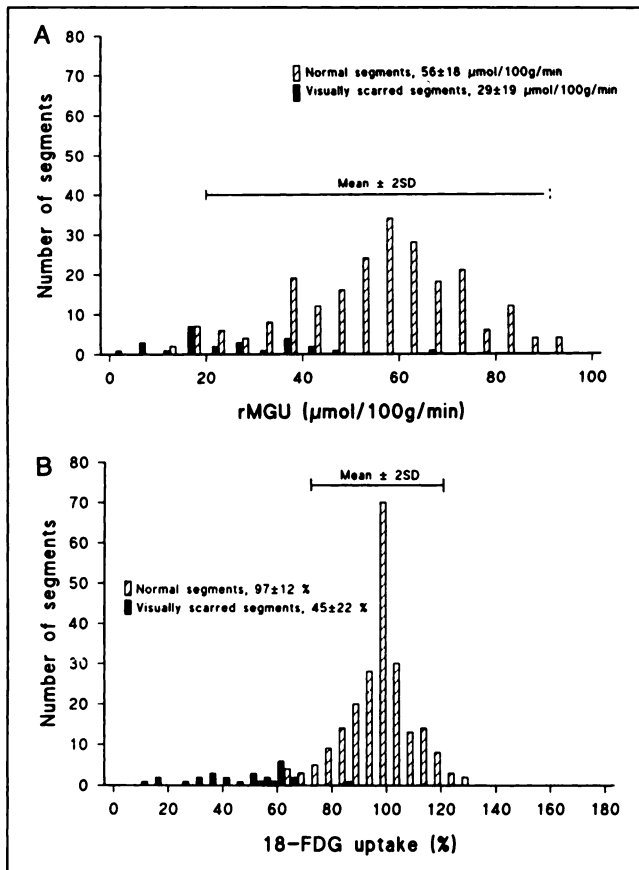
FIGURE 1. Distribution of rMGU (A) and [18F]FDG uptake (B) in normal and visually scarred segments. Note the wider range in normal segments and the higher overlap between the two segment groups in rMGU.

rMGU and [18F]FDG uptake were then found to be similar, and the parameters correlated highly with each other (r = 0.98).
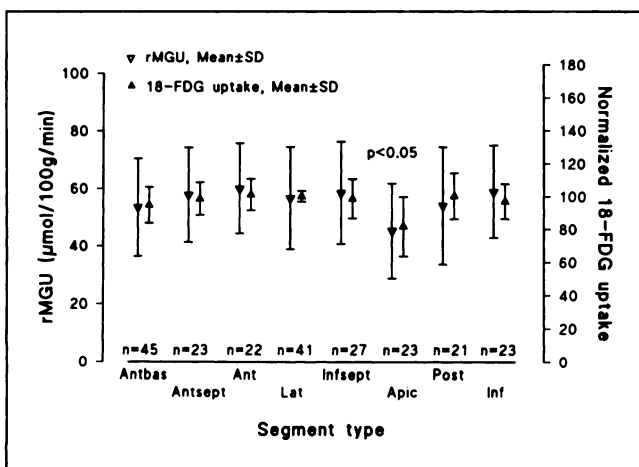

FIGURE 2. rMGU and [18F]FDG uptake in different types of normal segments. Values in apical segments were significantly lower than in other segments (p = 0.0001 in analysis of variance, p < 0.05 in Bonferroni test). Antbas = anterobasal; Antsept = anteroseptal; Ant = anterior; Lat = lateral; Infsept = inferoseptal; Apic = apical; Post = posterobasal; Inf = inferior.
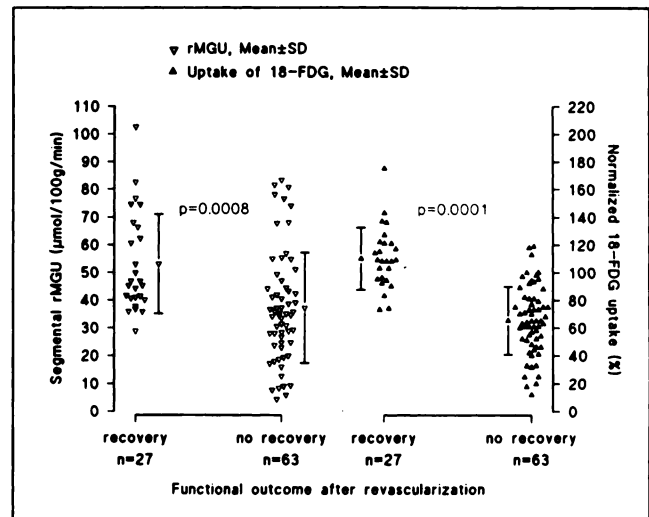

FIGURE 3. rMGU and [18F]FDG uptake in revascularized dysfunctional segments with and without recovery. Note the striking overlap in rMGU values between the two segment groups. P values between the segment groups were obtained by analysis of variance.

Fluorine-18-FDG Uptake and rMGU in Segments with Scarring

In 26 segments, scarring was detected by visual observation during coronary bypass surgery. Wall motion was abnormal in all the 26 segments by echocardiography and none of them recovered after the intervention. The rMGU and relative uptake of [18F]FDG were clearly reduced in these segments (29 ± 19 μmole/min/100 g and 45% ± 22%, p < 0.001 as compared with normal segments). However, the variability and overlap of values in normal and scarred segments was larger in rMGU than in relative [18F]FDG uptake (Fig. 1).

Fluorine-18-FDG Uptake, rMGU and Functional Recovery

In the 48 patients studied before and after revascularization by echocardiography, 106 (29%) segments were originally classified as dysfunctional at rest; 90 of these were subsequently revascularized. Wall motion improvement occurred in 27 (30%) of these segments. Segments without revascularization remained unchanged. Both the mean rMGU (53 ± 18 versus 37 ± 20 μmole/min/100 g, p = 0.0008) and the relative [18F]FDG uptake (110 ± 22% vs. 65 ± 24%, p = 0.0001) were significantly higher in segments that recovered compared to irreversibly dysfunctional segments (Fig. 3). The ability of both variables to distinguish between segments with and without recovery was tested by discriminant analysis. By using rMGU, 28% of segments were incorrectly classified in contrast to 17% by [18F]FDG uptake. Figure 4 demonstrates the effects of the cutoff values on the diagnostic performance of normalized [18F]FDG uptake and rMGU. Specificity was enhanced by higher limit values, but sensitivity decreased substantially. When 85%–90% of normalized [18F]FDG uptake was used as a threshold value, a sensitivity of 85% and specificity of 84% were reached simultaneously. However, with rMGU,
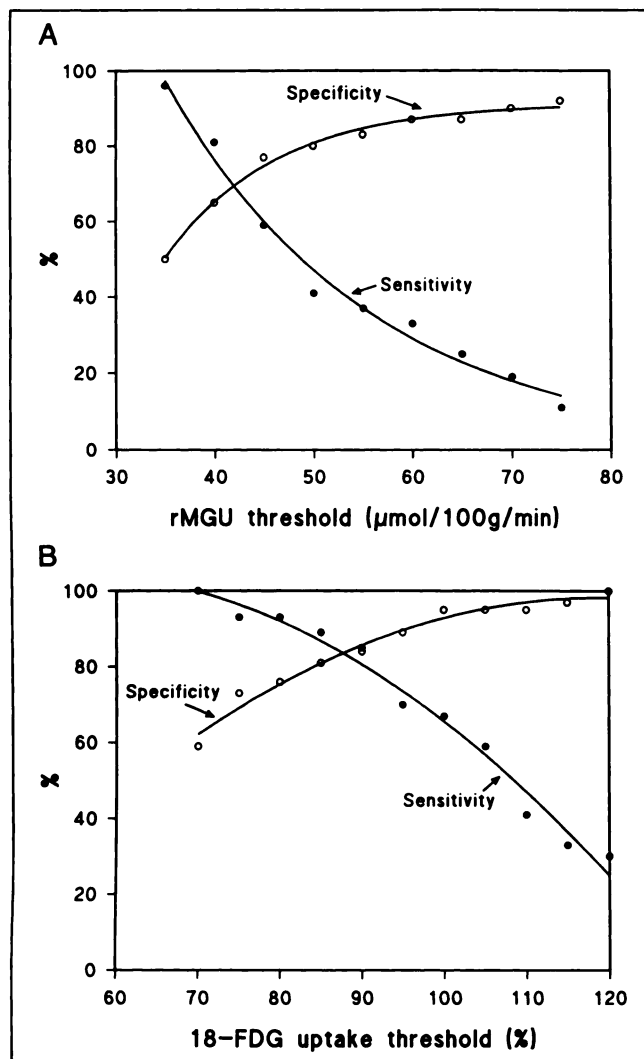
Quantitation of Glucose Uptake for Myocardial Viability • Knuuti et al.

2071

FIGURE 4. Sensitivity and specificity for recovery are shown as a function of the rMGU (A) and [18F]FDG uptake (B) threshold. Note that high sensitivity and specificity values cannot be obtained simultaneously by rMGU measurement.

such high sensitivity and specificity could not be obtained simultaneously. Again, relative rMGU values gave concordant results with relative [18F]FDG uptake.

Fluorine-18-FDG Uptake, rMGU, Resting Perfusion and Functional Recovery

SPECT perfusion results were available in 84 of the 90 initially dysfunctional revascularized segments (Fig. 5). The perfusion defects were classified as mild in 31 segments (normal in 5 segments), moderate in 17 segments and severe in 36 segments. Functional recovery was detected in 14 (45%), 6 (35%) and 5 (14%) segments, respectively. Significantly higher mean [18F]FDG uptake values were detected in the recovered segments as compared to the segments without recovery in the groups of moderate and severe SPECT perfusion defects (Fig. 5A). Positive and negative predictive values of preserved [18F]FDG uptake in these segments were 100% for wall motion recovery. In the group of mild perfusion defects, [18F]FDG uptake also

tended to be higher in the recovered segments than in the segments without recovery, but the difference was not statistically significant. In this group, none of the other methods could distinguish the recovered segments from the segments that did not recover.

The rMGU values were also higher in the segment groups that recovered as compared to those that did not (Fig. 5B). The difference was, however, statistically significant only in segments with severely decreased perfusion at rest. Also, the overlap of rMGU values in this group was large. Thus, it was not possible to distinguish recovered and nonrecovered segments in any perfusion defect group even by combined evaluation of rMGU and perfusion.

DISCUSSION

The results of this study show that semiquantitative relative [18F]FDG uptake is superior to calculated rMGU in predicting wall motion recovery after revascularization. The ability of rMGU to distinguish normal myocardium from scarred segments as well as segments with functional recovery from the irreversibly dysfunctional segments is deteriorated by the high variability of the glucose utilization rates between individuals.

rMGU per se or in combination with perfusion data was not able to accurately predict functional recovery in any of the segment groups (Figs. 4A, 5A). In contrast to this, acceptable good (~85%) sensitivity and specificity values were achievable with normalized [18F]FDG uptake alone (Fig. 4B). Evaluation of resting perfusion as studied by qualitative analysis of SPECT images showed that preserved normalized [18F]FDG uptake in the segments with moderate or severe perfusion defects at rest identified the recovered segments precisely (Fig. 5B). These results are concordant with most of the earlier studies showing that so-called mismatch of metabolism to blood flow predicts functional recovery (2,9,13). In the study by Gropler et al. (19), [18F]FDG uptake was not a good prognosticator for functional recovery. In that study, patients with recent myocardial infarctions were also included and the normalization and image analysis methods were different when compared to this and other previous studies.

rMGU variability in normal myocardium was notable and was caused mainly by variations between patients. In previous studies, the %s.d. of rMGU has been 26%–46% (13,18,29,36), and the s.d. of this study falls well within that range (31%). Interindividual and intraindividual variations have not been appreciated in the previous studies. Based on the data in previous studies, we calculated interindividual and intraindividual s.d.s; values ranged from 33% to 51% and 12% to 18%, respectively (18,23,36). In our recent study (29), the s.d.s were 26% and 9%, respectively, in a small population. The high interindividual variation of rMGU can be explained by several factors that regulate myocardial glucose uptake. These include myocardial workload, plasma levels of insulin and substrate supply, e.g., plasma levels of glucose and fatty acids, and
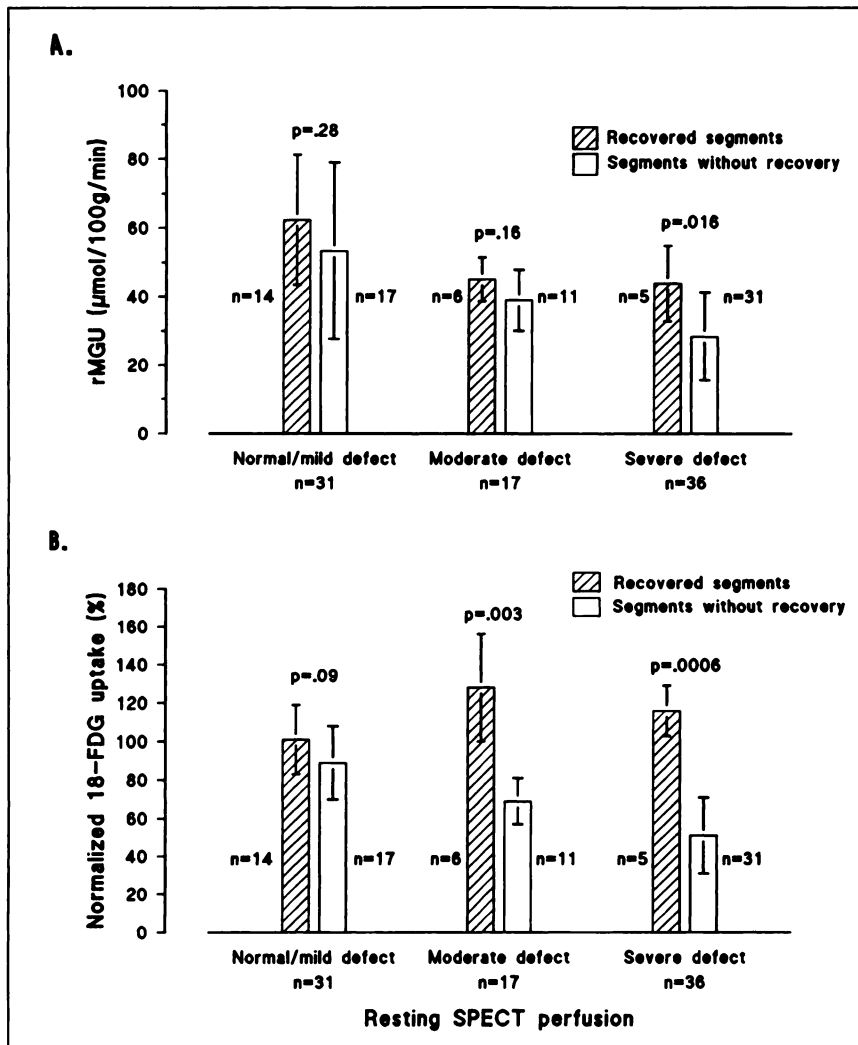
FIGURE 5. Relationship of rMGU (A) and [^{18}F]FDG uptake (B) to SPECT perfusion at rest and functional recovery. Data were available from 84 revascularized segments with abnormal wall motion. In five of these initially dysfunctional segments, SPECT perfusion was classified as normal.

oxygen supply (37,38). Plasma insulin and glucose levels can be standardized and matched by the glucose-insulin clamp technique (29,39). However, we have observed a similar degree of variability of rMGU in normal myocardial segments within and between patients during insulin clamp and after glucose loading (29).

The average value of absolute rMGU after glucose loading in normal segments in this study was 56 ± 18 μmole/min/100 g. In previous studies, rMGU has been 54 ± 29 μmole/min/100 g (calculated from the data of references 13,18,23,36). The rMGU values of scarred segments in previous studies have been more variable, depending on the criteria for selection of scarred segments (18,29,36). The ischemically injured myocardium has often been shown to be a mixture of living myocytes and scar tissue (4). In this study, the visually observed pale and firm area was taken as representing myocardial scar, and rMGU in these segments was 29 ± 19 μmole/min · 100 g. However, no biopsies were available to assess the amount of residual myocytes in these areas.

With normalization, the results are standardized to the segment with maximum perfusion. This results in reduced

interindividual variation of [^{18}F]FDG uptake and rMGU in normal segments. The drawbacks of the normalization method are the necessity of a flow study to localize the reference segments and that only relative and semiquantitative results are obtained. However, the method has clear advantages: static imaging is sufficient; analysis is simple; and no blood sampling is required. Therefore, the approach is more appropriate for clinical work. Intraindividual variability of rMGU and [^{18}F]FDG uptake in normal segments was only about 10%. Therefore, it can be assumed that the precise selection of a reference segment for normalization within normal myocardium is not critical to the results.

It is important to note that quantitation of rMGU gave no additional accuracy over [^{18}F]FDG uptake in predicting functional recovery when normalization was applied to both variables. However, there are several situations where quantitative measurement of rMGU is essential. For example, we have studied myocardial glucose consumption in diabetic patients and compared it to normal controls (40,41). We have also shown in vivo by [^{18}F]FDG PET that the glucose-free fatty acid cycle operates in the human heart (38). Thus, measurement of rMGU is required when

interest is focused on such questions as the influence of metabolic changes and medications on myocardial glucose uptake.

Resting perfusion alone, as studied by qualitative SPECT imaging, seems to underestimate viability as compared to [^{18}F]FDG uptake-flow relations. In some dysfunctional segments, perfusion was classified as mildly decreased of even normal at rest. None of the methods applied could distinguish the segments that recovered from those that did not in this segment group. However, preserved flow and metabolism in these segments per se show that considerable amount of viable tissue must reside in these segments, which may possibly be enough for clinical decision-making of viability and revascularization.

Potential Study Limitations

In SPECT perfusion imaging, both ^{201}Tl and ^{99m}Tc-MIBI were used and only a qualitative analysis of the SPECT images was performed. We think, however, that this is not an important problem since resting defect sizes have been shown to be similar if not identical with both tracers (42,43). In this study, absolute flow data were not available. We are therefore not able to compare our results to methods that use the ratio of [^{18}F]FDG and flow. Errors associated with Patlak graphical analysis are also possible and might explain at least part of the variation. These potential error sources include measurement of input functions and changes in plasma glucose levels after glucose loading. In our previous studies, however, reproducibility of rMGU measurements has been high, even in abnormal segments (29). In addition, changes in individual lumped constants cannot be accounted for in either normal or pathological myocardial tissue. This is also true for the dephosphorylation rate of [^{18}F]FDG phosphate, which has not been confirmed to be stable during ischemia and reperfusion.

CONCLUSIONS

Although rMGU measured by PET represents a physiologically meaningful signal, the high interindividual variability necessitates a wide reference range for normalcy and significantly reduces its diagnostic performance for viability. Normalization of myocardial [^{18}F]FDG uptake or rMGU to the area of maximal perfusion enhances the ability of [^{18}F]FDG PET to predict functional recovery. Accurate assessment of myocardial viability in clinical work can thus be achieved by static imaging and semiquantitative analysis.

ACKNOWLEDGMENTS

REFERENCES

1. Marshall RC, Tillisch JH, Phelps ME, et al. Identification and differentiation of resting myocardial ischemia and infarction in man with positron computed tomography, ^{18}F-labeled fluorodeoxyglucose and N-13 ammonia. *Circulation* 1983;67:766–788.
2. Tillisch J, Brunken R, Marshall R, et al. Reversibility of cardiac wall-motion abnormalities predicted by positron emission tomography. *N Engl J Med* 1986;314:884–888.
3. Schwaiger M, Brunken R, Grover-McKay M, et al. Regional myocardial metabolism in patients with acute myocardial infarction assessed by positron emission tomography. *J Am Coll Cardiol* 1986;8:800–808.
4. Brunken R, Tillisch J, Schwaiger M, et al. Regional perfusion, glucose metabolism, and wall motion in patients with chronic electrocardiographic Q-wave infarctions: evidence for persistence of viable tissue in some infarct regions by positron emission tomography. *Circulation* 1986;73:951–963.
5. Brunken RC, Schwaiger M, Grover-McKay M, Phelps ME, Tillisch J, Schelbert HR. Positron emission tomography detects metabolic activity in myocardial segments with persistent thallium perfusion defects. *J Am Coll Cardiol* 1987;10:557–567.
6. Tamaki N, Yonekura Y, Yamashita K, et al. Relation of left ventricular perfusion and wall motion with metabolic activity in persistent defects on thallium-201 tomography in healed myocardial infarction. *Am J Cardiol* 1988;62:202–208.
7. Fudo T, Kambara H, Hashimoto T, et al. F-18 deoxyglucose and stress N-13 ammonia positron emission tomography in anterior wall healed myocardial infarction. *Am J Cardiol* 1988;60:1191–1197.
8. Hashimoto T, Kambara H, Fudo T, et al. Non-Q-wave versus Q-wave myocardial infarction: regional myocardial metabolism and blood flow assessed by positron emission tomography. *J Am Coll Cardiol* 1988;12:88–93.
9. Tamaki N, Yoshiharu Y, Yamashita K, et al. Positron emission tomography using fluorine-18 deoxyglucose in evaluation of coronary artery bypass grafting. *Am J Cardiol* 1989;64:860–865.
10. Brunken RC, Kottou S, Nienaber CA, et al. PET detection of viable tissue in myocardial segments with persistent defects at Tl-201 SPECT. *Radiology* 1989;172:65–73.
11. Tamaki N, Ohtani H, Yamashita K, et al. Metabolic activity in the areas of new fill-in after thallium-201 reinfection: comparison with positron emission tomography using fluorine-18-deoxyglucose. *J Nucl Med* 1991;32:673–678.
12. Bonow RO, Dilsizian V, Cuocolo A, Bacharach SL. Identification of viable myocardium in patients with chronic coronary artery disease and left ventricular dysfunction. Comparison of thallium scintigraphy with reinjection and PET imaging with ^{18}F-fluorodeoxyglucose. *Circulation* 1991;83:26–37.
13. Nienaber CA, Brunken RC, Sherman CT, et al. Metabolic and functional recovery of ischemic human myocardium after coronary angioplasty. *J Am Coll Cardiol* 1991;18:966–978.
14. Altehoefer C, Kaiser H-J, Dörr R, et al. Fluorine-18 deoxyglucose PET for assessment of viable myocardium in perfusion defects in ^{99m}Tc-MIBI SPET: a comparative study in patients with coronary artery disease. *Eur J Nucl Med* 1992;19:334–342.
15. Marwick TH, MacIntyre WJ, Lafont A, Nemec JJ, Salcedo EE. Metabolic responses of hibernating and infarcted myocardium to revascularization: a follow-up study of regional perfusion, function and metabolism. *Circulation* 1992;85:1347–1353.
16. Perrone-Filardi P, Bacharach SL, Dilsizian V, et al. Metabolic evidence of viable myocardium in regions with reduced wall thickness and absent wall thickening in patients with chronic ischemic left ventricular dysfunction. *J Am Coll Cardiol* 1992;20:161–168.
17. Porenta G, Kuhle W, Czernin J, et al. Semiquantitative assessment of myocardial blood flow and viability using polar map displays of cardiac PET images. *J Nucl Med* 1992;33:1623–1631.
18. Vanoverschelde J-L, Melin JA, Bol A, et al. Regional oxidative metabolism in patients after recovery from reperfused anterior myocardial infarction: relation to regional blood flow and glucose uptake. *Circulation* 1992;85:9–21.
19. Gropler RJ, Geltman EM, Sampathkumaran K, et al. Functional recovery after coronary revascularization for chronic coronary artery disease is dependent on maintenance of oxidative metabolism. *J Am Coll Cardiol* 1992; 20:569–577.
20. Sokoloff L, Reivich M, Kennedy C, et al. The ^{14}C-deoxyglucose method for the measurement of local cerebral glucose utilization: theory, procedure and

normal values in the conscious and anesthetized albino rats. *J Neurochem* 1977;28:897–916.

21. Phelps ME, Huang SC, Hoffman EJ, Selin C, Sokoloff L, Kuhl DE. Tomographic measurement of local cerebral glucose metabolic rate in humans with (F-18)2-fluoro-2-deoxy-D-glucose: Validation of method. *Ann Neurol* 1979;6:371–388.

22. Patlak CS, Blasberg RG. Graphical evaluation of blood-to-brain transfer constants from multiple-time uptake data. Generalizations. *J Cereb Blood Flow Metab* 1985;5:584–590.

23. Gambhir SS, Schwaiger M, Huang S-C, et al. A simple noninvasive quantification method for measuring myocardial glucose utilization in humans employing positron emission tomography and ^{18}F-deoxyglucose. *J Nucl Med* 1989;30:359–366.

24. Hamacher K, Coenen HH, Stöcklin G. Efficient stereospecific synthesis of no-carrier-added 2-[^{18}F]-fluoro-2-deoxy-D-glucose using aminopolyether supported nucleophilic substitution. *J Nucl Med* 1986;27:235–238.

25. Solin O, Bergman J, Haaparanta M, Reissell A. Production of ^{18}F from water targets specific radioactivity and anionic contaminants. *Radiat Isot* 1988;39:1065–1071.

26. Bergman J, Aho K, Haaparanta M, Reissell A, Solin O. Production of ^{18}F$^-$ from H$_2$O: specific radioactivity and chemical reactivity. *J Lab Comp Radiopharm* 1989;26:143–145.

27. Henze E, Huang SC, Ratib O, Hoffman E, Phelps ME, Schelbert HR. Measurements of regional tissue and blood-pool radiotracer concentrations from serial tomographic images of the heart. *J Nucl Med* 1983;24:987–996.

28. Hoffman EJ, Huang S-C, Phelps ME. Quantitation in positron emission tomography: 1. Effect of object size. *J Comput Assist Tomogr* 1979;3:299–308.

29. Knuuti MJ, Nuutila P, Ruotsalainen U, et al. Euglycemic hyperinsulinemic clamp and oral glucose load in stimulating myocardial glucose utilization during positron emission tomography. *J Nucl Med* 1992;33:1255–1262.

30. Ratib O, Phelps ME, Huang S-C, Henze E, Selin CE, Schelbert HR. Positron tomography with deoxyglucose for estimating local myocardial glucose metabolism. *J Nucl Med* 1982;23:577–586.

31. Krivokapich J, Huang SC, Phelps ME, et al. Estimation of rabbit myocardial metabolic rate for glucose using fluorodeoxyglucose. *Am J Physiol* 1982;243:H884–H895.

32. Krivokapich J, Huang SC, Selin CE, Phelps ME. Fluorodeoxyglucose rate constants, lumped constant, and glucose metabolic rate in rabbit heart. *Am J Physiol* 1987;252:H777–H787.

33. Schiller NB, Shah PM, Crawford M, et al. Recommendations for quantitation of the left ventricle by two-dimensional echocardiography. *J Am Soc Echo* 1989;2:358–367.

34. Kerber R, Litchfield R. Postoperative abnormalities of interventricular septal motion: two-dimensional and M-mode echocardiographic correlations. *Am Heart J* 1982;104:263–268.

35. Kadish AH, Little RL, Sternberg JC. A new and rapid method for the determination of glucose by measurement of rate of oxygen consumption. *Clin Chem* 1968;14:116–131.

36. Choi Y, Hawkins RA, Huang S-C, et al. Parametric images of myocardial metabolic rate of glucose generated from dynamic cardiac PET and 2-[^{18}F]Fluoro-2-deoxy-d-glucose studies. *J Nucl Med* 1991;32:733–738.

37. Camici P, Ferranini E, Opie LH. Myocardial metabolism in ischemic heart disease: basic principles and application to imaging by positron emission tomography. *Prog Cardiovasc Dis* 1989;32:217–238.

38. Nuutila P, Koivisto VA, Knuuti MJ, et al. The glucose-free fatty acid cycle operates in human heart and skeletal muscle in vivo. *J Clin Invest* 1992;89:1767–1774.

39. Hicks RJ, Herman WH, Kalff V, et al. Quantitative evaluation of regional substrate metabolism in the human heart by positron emission tomography. *J Am Coll Cardiol* 1991;18:101–111.

40. Nuutila P, Knuuti J, Ruotsalainen U, et al. Glucose uptake in myocardial and skeletal muscle with positron emission tomography (PET) in type 2 diabetes [Abstract]. *Diabetology* 1990;33(suppl):A23.

41. Nuutila P, Knuuti J, Ruotsalainen U, et al. Insulin resistance is localized to skeletal but not heart muscle in type I diabetes. *Am J Physiol* 1993;264 (*Endocrinol Metab* 27):E756–E762.

42. Narahara KA, Villanueva-Meyer J, Thompson CJ, Brizendine M, Mena I. Comparison of thallium-201 and technetium-99m hexakis 2-methoxyisobutyl of myocardial ischemia and infarction in coronary artery disease. *Am J Cardiol* 1990;66:1438–1444.

43. Maublant JC, Marcaggi X, Lusson JR, et al. Comparison between thallium-201 and technetium-99m methoxyisobutyl exercise and redistribution in coronary artery disease. *Am J Cardiol* 1992;69:183–187.